# LATTICE LOCATION STUDIES OF HEAVY IONS IMPLANTED IN MAGNESIUM

M. R. DA SILVA, A. MELO and J. C. SOARES
Centro de Física Nuclear da Universidade de Lisboa, Portugal

E. ALVES and M. F. DA SILVA
Departamento de Física, LNETI, Sacavém, Portugal

P. M. J. WINAND and R. VIANDEN
Institut für Strahlen und Kernphysik, University of Bonn, FRG

*(Received 19 October 1983)*

*ABSTRACT* — The Rutherford backscattering channeling technique has been used to study the quality of magnesium single crystals for lattice location measurements. First results using Hf, Au, Tl and Pb atoms implanted in magnesium are presented and discussed. Particular relevance is given to the experimental set-up.

## 1 — INTRODUCTION

It is well known that defects such as vacancies or interstitials might modify many properties of materials. In most of the cases, however, it is not possible to predict the result of the creation of defects or their behaviour under various parameters like the temperature.

Defects might be introduced in materials using classical methods. Ion implantation, however, increasingly used in recent years, has become a more powerful and versatile alternative. In particular, it allows the simulation of production of unwanted effects present in research and power reactors and in the walls of plasma containers used in the development of fusion reactors.

In the present work the first results of a systematic investigation of defects in magnesium are presented. The defects are

introduced by implanting heavy ions in magnesium single crystals, and the Rutherford backscattering-channeling technique is used for the analysis.

Special relevance is given in this work to the experimental apparatus and analysing technique, including the preparation of samples, the orientation of the single crystals and the location of the implanted impurities.

Preliminary results obtained with the Hf, Au, Tl, and Pb impurities implanted in magnesium are presented and discussed.

## 2 — MEASUREMENT TECHNIQUE AND EXPERIMENTAL PROCEDURE

### 2.1 — *The Rutherford-Backscattering (RBS) / Channeling Technique*

If a beam of positive ions with energy $E_0$ impinges on the surface of a solid, Rutherford scattering occurs and the energy

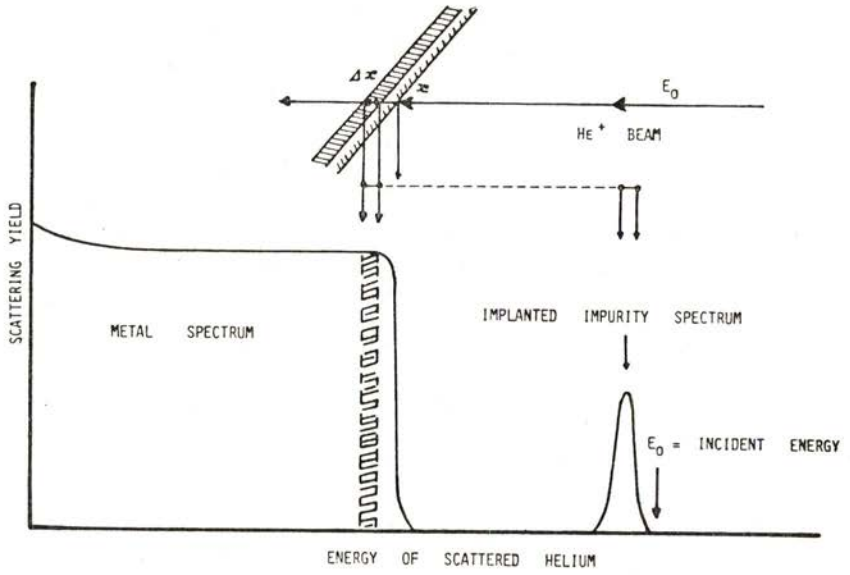


Fig. 1 — Schematic diagram of the He+ backscattered from a light metal implanted with a heavy impurity.

of the particles scattered at an angle relative to the beam direction is given by $E = k^2 E_0$. The kinematic factor, k, depends on the scattering angle and on the masses of the incident beam and target atoms.

Fig. 1 shows, schematically, the energy spectrum of $He^+$ ions scattered from the surface of a metal implanted with a heavy impurity.

The strong dependence of E on the mass of the scattering nucleus makes the RBS technique very useful to distinguish different elements in the near surface region of the solids. Further, the continuous energy loss of the in and outgoing ions, mainly due to the interaction with the electrons of the solid, allows the conversion of the energy scale to a depth scale. Thus, depth profiles of impurities in solids can easily be obtained.

If in the magnesium crystal heavy impurities like Hf, Au, Pb or Tl are dissolved, the ions scattered from these impurities have higher energies than those scattered from the Mg atoms making this method very sensitive for the qualitative and quantitative analysis of these impurities. For impurities concentrated in a layer near the surface, this technique gives with accuracy the thickness of the layer and the depth at which the layer is located [1].

Atoms lighter than magnesium, like oxygen and carbon, can also be detected with this technique. However, the sensitivity is poorer due to the lower Rutherford yield and to the fact that these impurities appear as peaks superimposed on a continuous magnesium RBS spectrum.

Fig. 2 shows RBS spectra of a magnesium single crystal with implanted lead. Apart from impurities like Si, P and Ca, it can be seen that at the surface of the magnesium two thin layers of oxygen and carbon are present and their thicknesses are calculated to be less than 100 Å.

When a sufficiently collimated ion beam is directed along a major symmetry direction of a single crystal, like the $< 11\bar{2}0 >$ axis of the Mg crystal shown in Fig. 2, a strong reduction of the Rutherford backscattering yield is observed. This is due to a reduced collision probability of the ions with the target nuclei. The repulsive potential of the lattice atoms steers the ions which

have a very low transverse momentum away from the rows or planes of the crystal atoms. This phenomenon is called the «Channeling effect» [2].

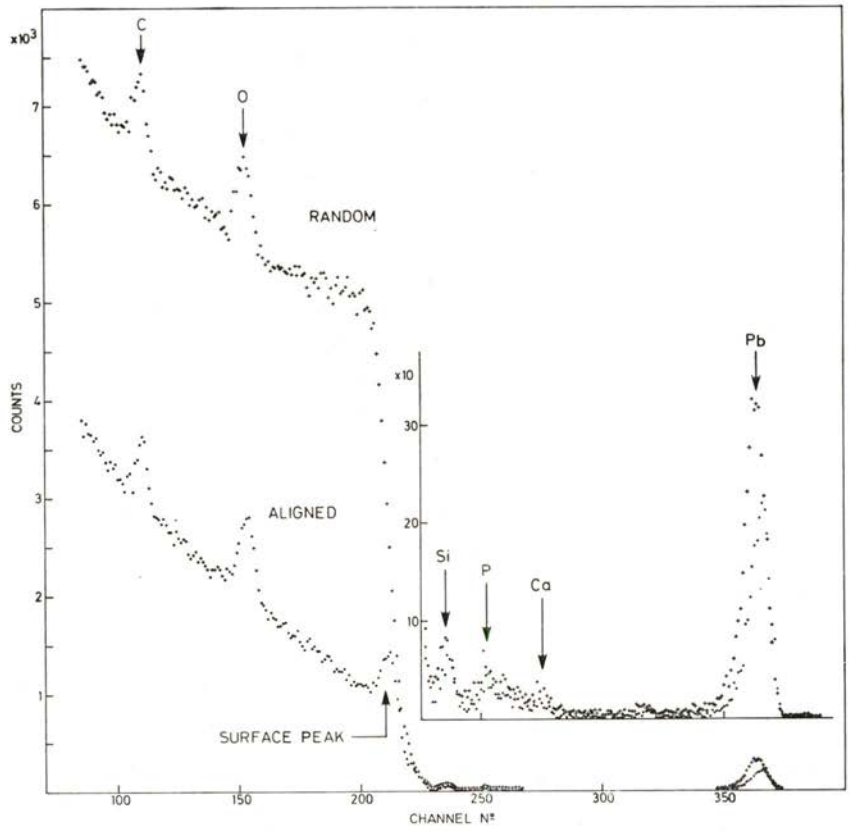


Fig. 2 — RBS spectra of a magnesium single crystal under ramdom and aligned orientation with respect to the beam axis.

## 2.2 — *Sample preparation*

The magnesium samples used in this work were 12 mm diameter by 2 mm thick disks, spark cut approximately normal to the axis $< 10\bar{1}0 >$ of a magnesium single crystal. They were cleaned by chemical etching in $HNO_3$ (65 %, P. A.), rinsed with water and dried.

The quality of the crystals was studied with the RBS channeling technique. From typical spectra as shown in Fig. 2, the concentration of the impurities remaining in the sample after cleaning can be obtained. Most of these residual impurities do not interfere with the heavy implanted impurities we intend to study in this work.

The implantation of the single crystals was performed using the electromagnetic mass separator of the Institut für Strahlen-und Kernphysik der Universität Bonn. The magnesium crystal was mounted on a support isolated from the implanting chamber evacuated to a pressure better than $5 \times 10^{-6}$ mbar. During the implantation, the ion beam current was controlled and kept as low as possible to reduce heating effects on the crystals. The standard implantation energy used in this work was 80 keV for single charged ions. The implanted doses were in the range of 1 to $5 \times 10^{14}$ atom/cm$^2$. Some samples implanted with the highest dose showed some darkening at the surface after implantation.

### 2.3 — *Experimental set-up*

The measurements were performed at the 2 MeV Van de Graaff accelerator of the LNETI, Sacavém. The 1.2 MeV $He^+$ beam is collimated by two circular tantalum diaphragms (1 mm diameter) at a distance of 230 cm. The maximum beam divergence is 0.045° and the beam spot size at the target about 1 mm$^2$. The beam current is kept at a value of the order of $4 \times 10^{-9}$ A to avoid radiation damage of the crystal during the measurements.

The samples are mounted in a two axis goniometer described below, located inside the scattering chamber (Fig. 3). This chamber is evacuated by means of a turbo-molecular pump to a pressure better than $10^{-6}$ mbar. The sample holder is surrounded by a copper shield cooled to liquid nitrogen temperature to reduce surface contamination during the experiment. A secondary electron suppression shield around the sample allows an accurate charge measurement by integration of the beam current on the sample.

The backscattered particles are counted with two silicon surface barrier detectors: a 100 mm$^2$ annular detector placed at 180° with an energy resolution of about 25 keV, and a 50 mm$^2$

detector positioned at a scattering angle of 140° and with a resolution of 15 keV. The signals of both detectors are analysed and stored in a multichannel analyser with pile up rejection facilities.

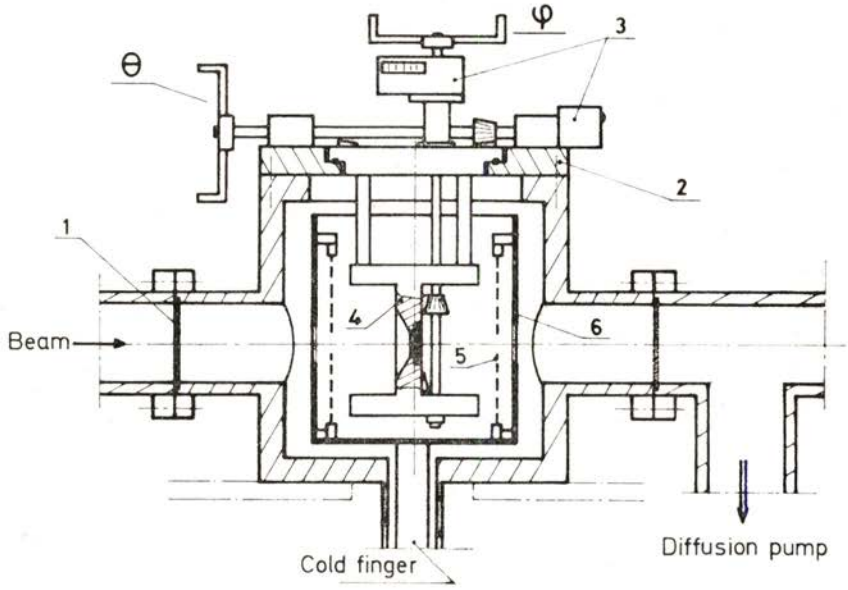


Fig. 3 — Scattering chamber: 1. diaphragm; 2. chamber lid with the goniometer; 3. $\theta$ and $\varphi$ counters; 4. sample holder; 5. electrostatic shield; 6. thermal shield.

The two axis goniometer built at the ISKP-Bonn University allows the orientation of the single crystals with respect to the beam direction with a positional accuracy of 0.01° around the vertical axis and 0.02° around the horizontal axis. This goniometer, shown in Fig. 4, allows tilt motions of 360° around the two axes. The settings are read in two mechanical counters. The linearity of the counters and the accuracy to reproduce a setting better than 0.01° was tested using a laser beam reflected in a mirror mounted in the position of the sample. With this goniometer the crystal can be set in different orientations relative to the direction of the incident collimated beam. When rotating the crystal around the vertical axis the only restriction is the shadow of the crystal support on the particle detectors. A rotation of 180° around the vertical axis is particularly useful for investigations using not too

thick crystals. After this rotation the backside of the crystal can be studied and the accuracy of the goniometer can be tested.

The zero of the goniometer, $\theta = 0$, is defined as the angle in which both the direction of the beam and the rotation axis are coincident. This zero has been determined by two different methods: a) using a front silvered mirror mounted in the sample

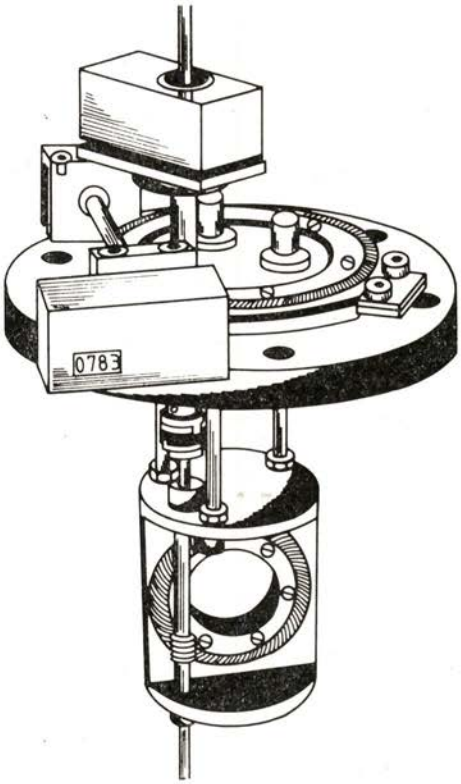


Fig. 4 — Goniometer built at the ISKP — Bonn University with drawings from M. A. Augustiniak (Bell Lab.) adapted by W. Schaub (ISKP).

holder and with the aid of a theodolit, a "pin point" was aligned with the beam. The $\theta = 0$ position was the one when both the "pin point" and its image were coincident in the theodolit axis; b) the other method was based on the fact that the same channeling direction is found when the crystal orientation is changed from $(\theta, \varphi)$ to $(-\theta, \varphi + 180^{\circ})$. Fig. 5 shows the

results of these measurements for the (0001) symmetry plane of a magnesium crystal.

With both methods the same zero value was found with an accuracy of 0.02°.

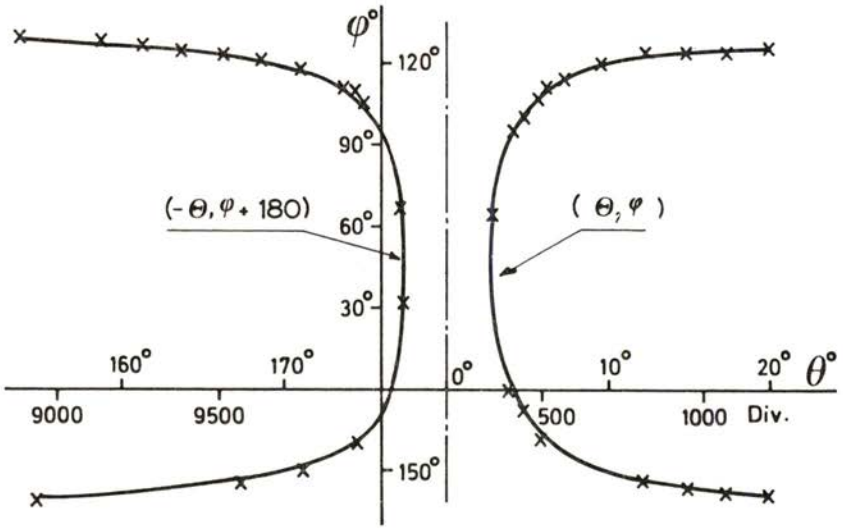


Fig. 5 — Coordinates of the (0001) plane near normal incidence for $+\theta$ and $-\theta$.

## 2.4 — *Experimental Procedure*

Typical energy spectra of $He^+$ ions backscattered from a Mg single crystal are shown in Fig. 2, for a random and for a major symmetry direction. The aligned spectrum shows clearly the so called "surface peak" due to the first atomic layers of the crystal.

In channeling measurements windows are set in the RBS spectra to select particles scattered from the implanted impurity and from the magnesium host at the depth of the implanted layer.

The RBS yield of the Mg host, inside the window, as a function of the angle between a crystalographic direction and the beam direction shows a dip with a minimum in the channeling direction (Fig. 6). The yield at this minimum relative to a random yield is the $\chi_{min}$. The critical angle, $\psi_{1/2}$, is determined from the

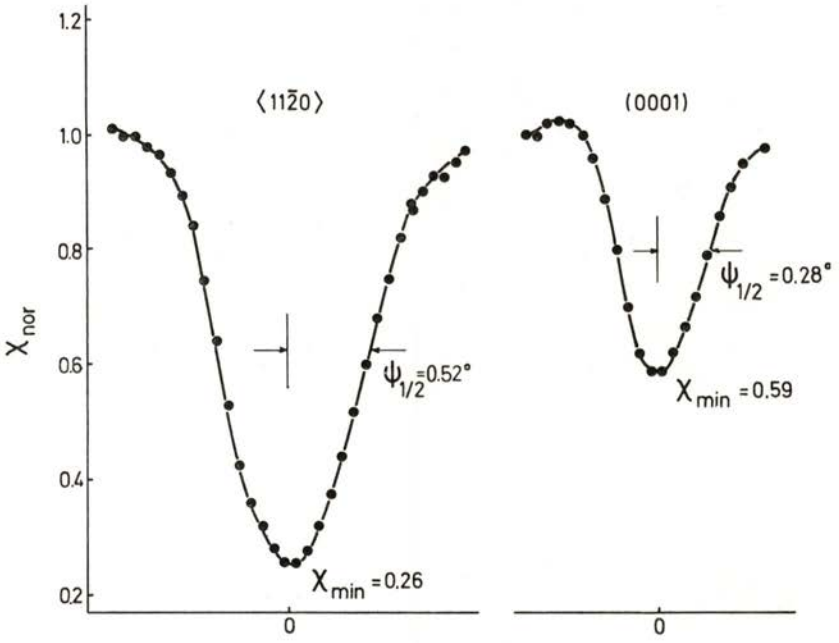


Fig. 6 — Axial and planar angular scans for the not implanted magnesium single crystal.

channeling angular scan by the half width at a level halfway between the minimum yield and the random level. These parameters, $\chi_{min}$ and $\psi_{1/2}$, are two characteristic quantities for channeling. They give information on the quality of the crystal and on the lattice location of impurities. The smaller $\chi_{min}$ is, the more perfect is the crystal. Any perturbation of the lattice will increase $\chi_{min}$. The angle $\psi_{1/2}$ characterizes the "openness" of the channel.

To control possible effects of radiation damage and surface contamination of the crystal during the measurement sequence, the scans are normally done in two halves comparing the minimum yield obtained at the beginning with that at the end of the scan. Corrections are made, when necessary, for the shift in the energy, due to the accumulation of a carbon layer at the surface, during the experiment.

The comparison of the measured dips with the theoretical predictions [3] gives information on the crystal lattice perfection

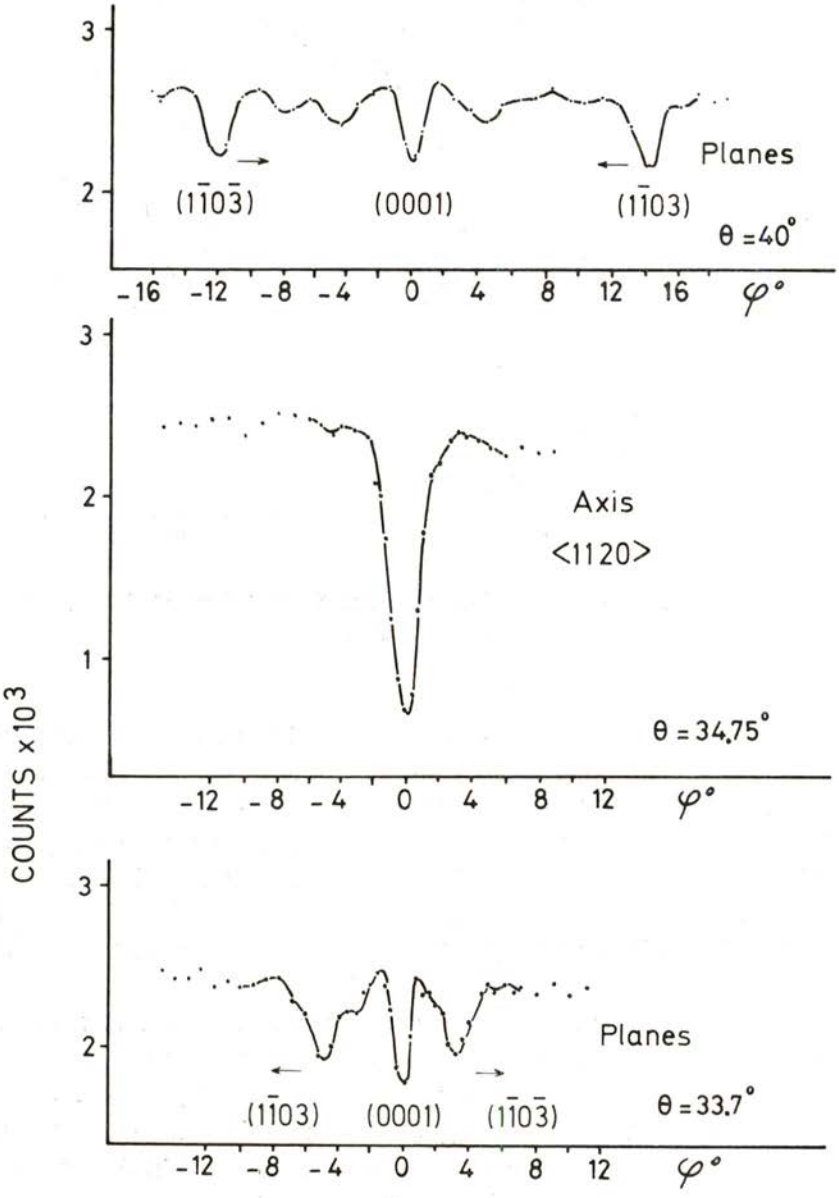


Fig. 7 *a*) — Scan for three different values of $\theta$; yields not normalized.

and on the experimental set-up misalignment. The comparison of the dips corresponding to the single crystal with those of the implanted impurities gives information about the impurity location in the crystal matrix.

In a lattice location measurement the first step is to orientate the single crystal with respect to the beam direction. Though not essential, it is useful to know the approximate orientation of a major axis prior to the alignment of the crystal. This information can be obtained from X-ray diffraction measurements. In this circumstance the procedure to find one axial direction (in this case the $<11\bar{2}0>$ axis of the Mg crystal) is schematically represented in Fig. 7a. For two positions of constant $\theta$ ( $\theta_1 = 40°$, $\theta_2 = 33.7°$ ) a scan is done by varying $\varphi$. Several planar dips are seen corresponding to the ( $1\bar{1}0\bar{3}$ ), ( 0001 ) and ( $1\bar{1}03$ ) planes. The intersection of these planes on a stereographic projection determines the location of the $<11\bar{2}0>$ axis which is confirmed by the axial angular scan as represented in Fig. 7b.

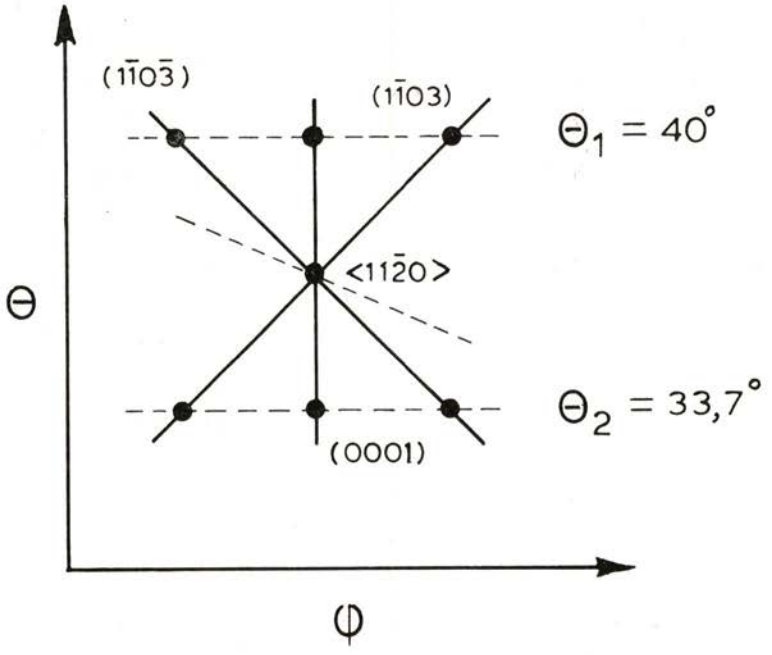


Fig. 7 *b*) — Stereographic projection to find the $<11\bar{2}0>$ coordinates.

The correct identification of other axes is confirmed by the agreement of the calculated values with the experimental ones for the angles between the axes. The stereographic projection of the main directions found for the magnesium crystal, which belongs to the hexagonal closed packed (hcp) configuration, is shown in Fig. 8.

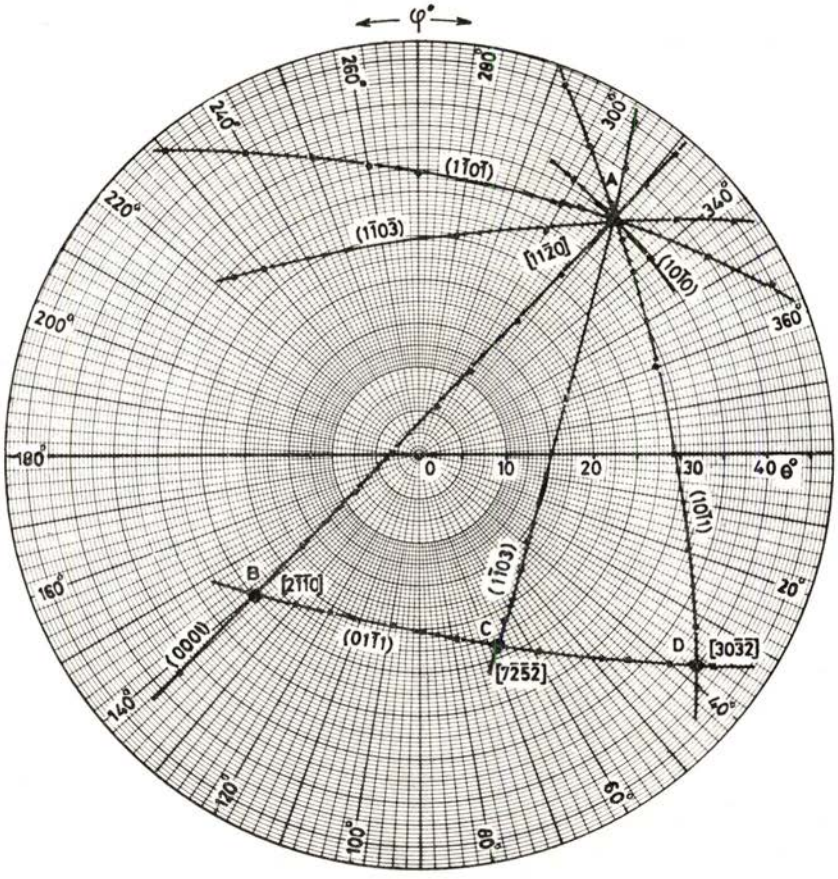


Fig. 8 — Stereographic projection of the main directions for the magnesium crystal.

## 3 — RESULTS AND DISCUSSION

Table 1 shows the channeling parameters obtained for several crystalographic directions of the magnesium single crystal. The theoretical predictions are also included for comparison. There is a fair agreement for the $\psi_{1/2}$ parameter. The high values obtained for $\chi_{min}$ means the existence of some disorder at the magnesium surface. In particular, the observed layers of carbon and oxygen can explain this fact. However, the magnesium crystal shows enough quality for studies of defects using ion implanted heavy impurities.

Experimental and theoretical values of channeling parameters for the magnesium single crystal

| | $\psi_{1/2}$ | | $\chi_{min}$ | |
|---|---|---|---|---|
| | Exp. | Theor. | Exp. | Theor. |
| $< 11\bar{2}0 >$ | 0.52 ± 0.05 | 0.59 | 0.26 ± 0.05 | 0.05 |
| $< 10\bar{1}0 >$ | 0.48 ± 0.05 | 0.45 | 0.35 ± 0.06 | 0.08 |
| (0001) | 0.28 ± 0.03 | 0.28 | 0.59 ± 0.10 | 0.26 |

The measured axial and planar angular scans for Hf and Pb are shown in Fig. 9, 10 and 11. The data are normalized such that the average value of the scattered yield off the channeling direction is unity.

The good coincidence between the Hf and the Mg scans for the major directions (Fig. 9) indicate total occupancy of substitutional sites by the Hf atoms in the host lattice.

This does not occur with the lead impurity (Fig. 10). Similar scans along the $< 10\bar{1}0 >$ axial direction and the $(10\bar{1}0)$ plane shown in Fig. 11 were also measured. These results indicate that only a fraction of about 50 % of lead impurity is substitutional in magnesium. The remaining fraction is probably randomly located in the oxide layer at the magnesium surface.

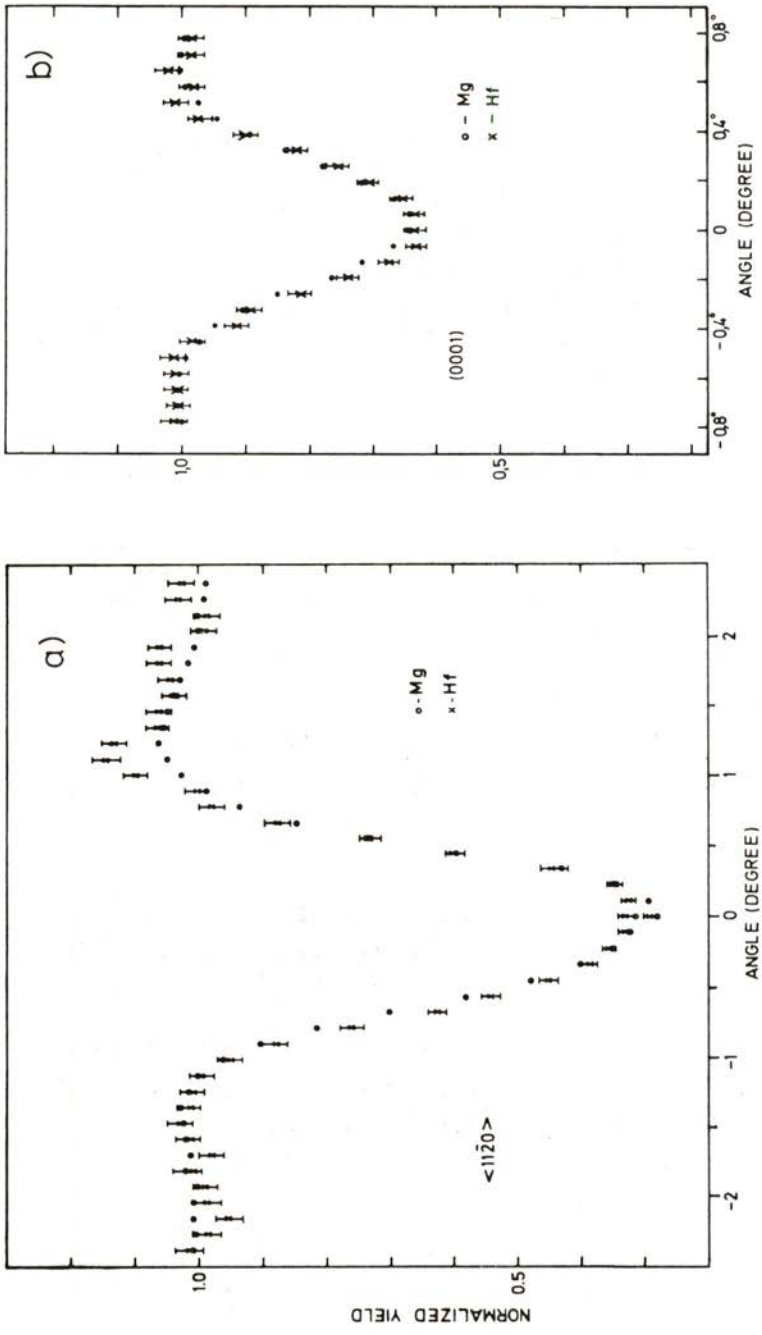


Fig. 9 — *a*) Angular scan curves along the <11$\bar{2}$0> axial direction for Hf in Mg. *b*) idem for the (0001) plane

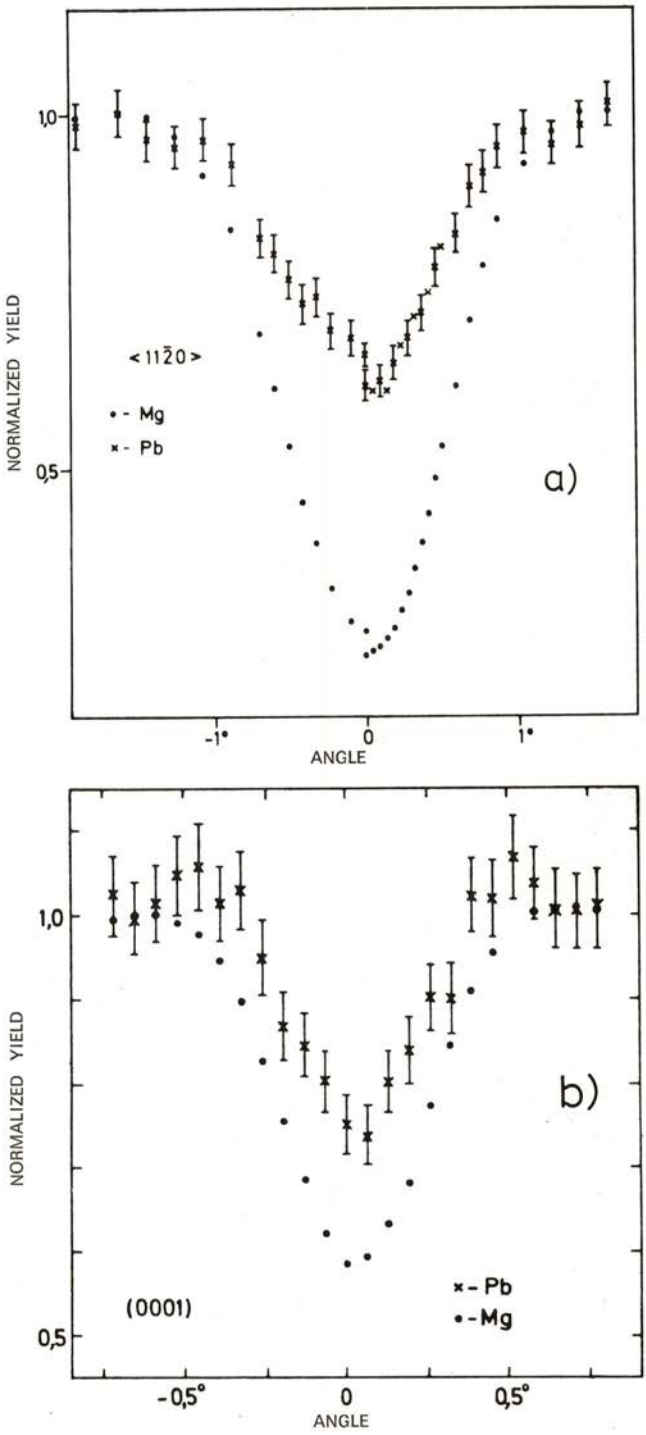


Fig. 10 — *a*) Angular scan curves along the <11$\bar{2}$0> axial direction for Pb in Mg. *b*) idem for the (0001) plane.

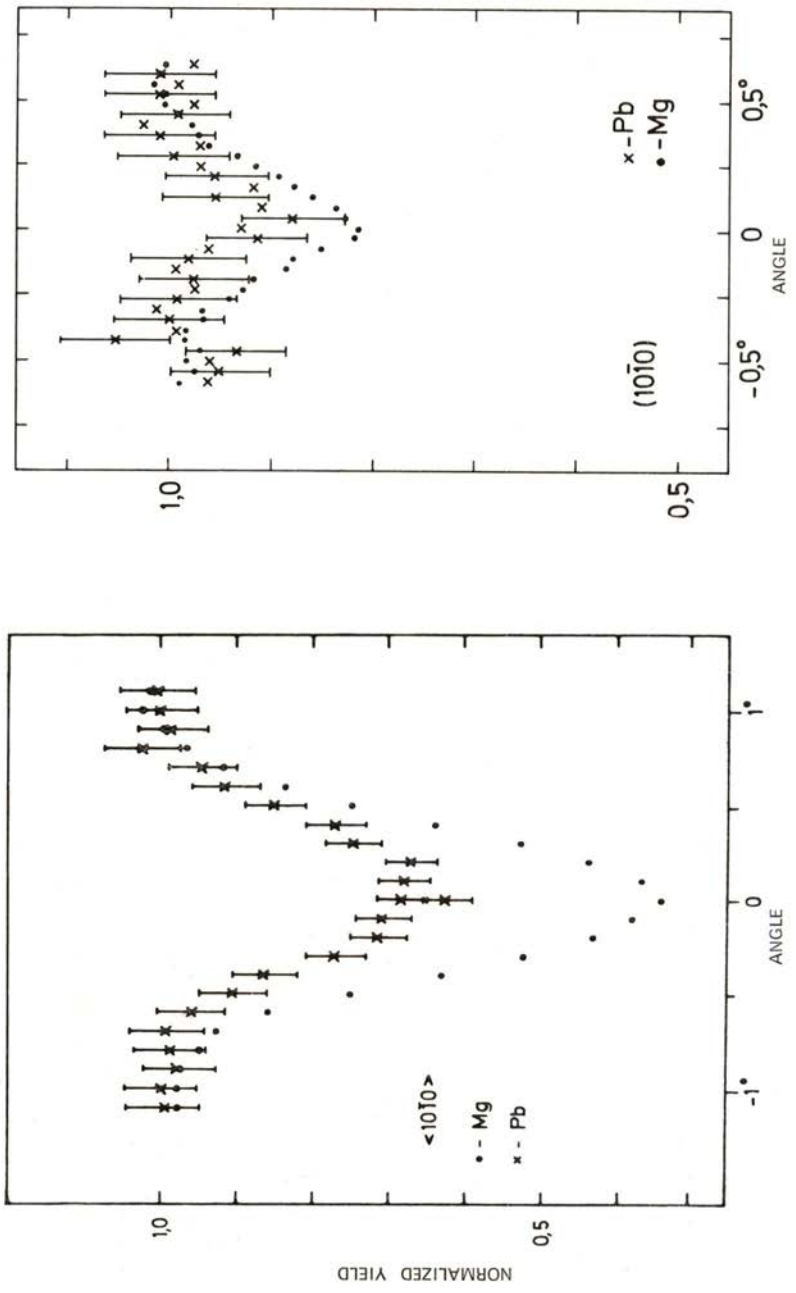


Fig. 11 — *a*) Angular scan curves along the <10$\bar{1}$0> axial direction for Pb in Mg. *b*) idem for the (10$\bar{1}$0) plane.

Completely different results were obtained for Au in Mg (Fig. 12). Small substitutionality was observed in the $< 11\bar{2}0 >$ axial direction while almost complete substitutionality was observed along the ( 0001 ) plane. These results may indicate that gold is interstitially located in the magnesium lattice.

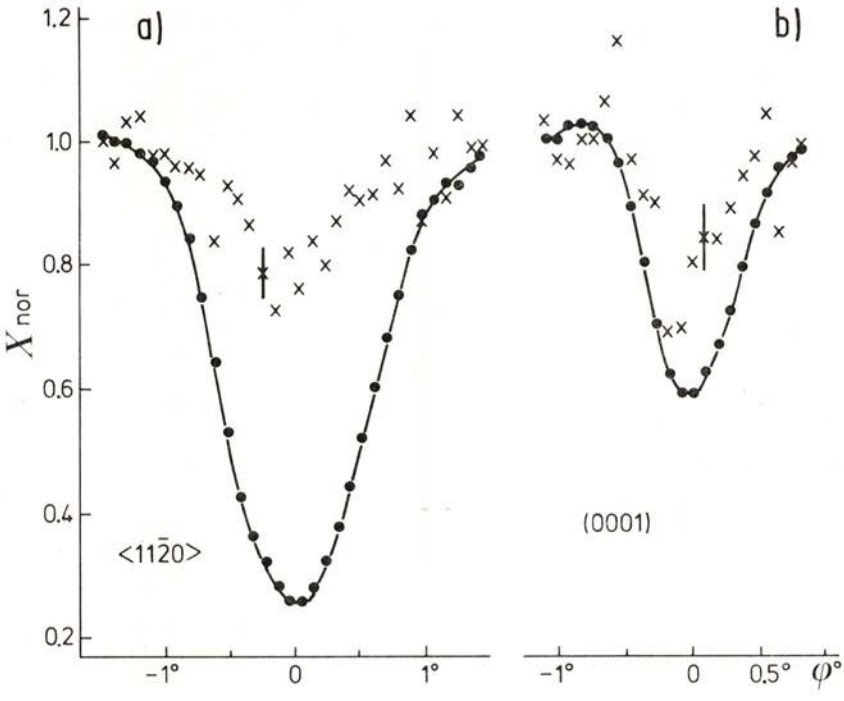


Fig. 12 — *a*) Angular scan curves along the <1120> axial direction for Au in Mg. *b*) idem for the (0001) plane ( • Mg; × Au).

Fig. 13 shows preliminary results for the Tl impurity. The small substitutionality observed in the $< 11\bar{2}0 >$ direction might indicate either that Tl is interstitially located in Mg or that during the implantation it segregates to the surface.

Further measurements, will be done with better statistics and in other directions to improve the quality of these results.

In order to test theoretical predictions [4, 5, 6] this work will be pursued using other impurities implated in Mg. Similar

measurements are also planned using higher implantation energies before and after annealing treatment of the samples.

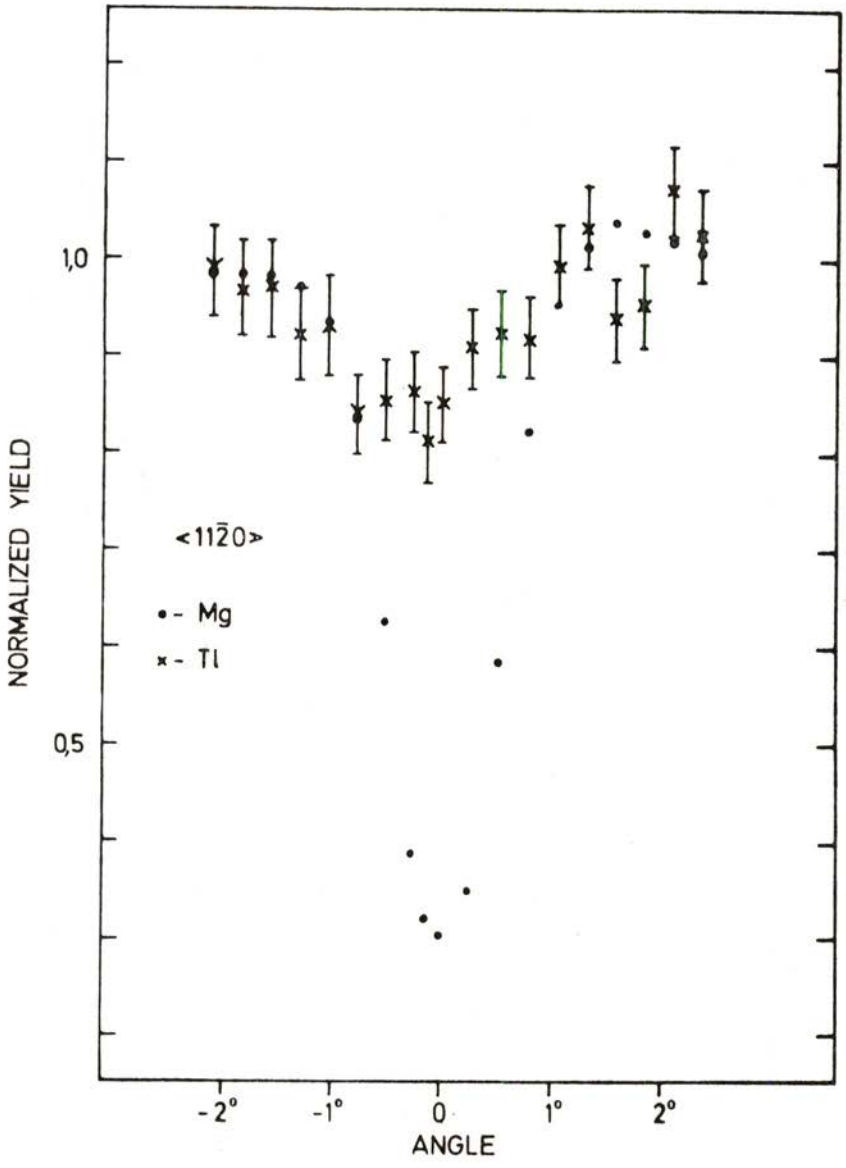


Fig. 13 — Angular scan curve along <11$\bar{2}$0> axial direction for Tl in Mg.

This work was partially suported by JNICT under contract N° 426.82.83 and by GTZ (F. R. Germany).

One of us (J. C. Soares) would like to thank Professor Dr. E. Bodenstedt for his hospitality during the execution of the implantations, Dr. K. Freitag for helpful discussions, and the Alexander von Humboldt Foundation (Bonn) for supporting the stay at the Institut für Strahlen und Kernphysik der Universität Bonn. J. Winand and R. Vianden acknowledge the DAAD for financial support during their stay in the CFNUL and in the LNETI.

We thank M. Lança e Silva for his help in running the accelerator.

## REFERENCES

[1] W. K. CHU in «*Uses of Low Energy Accelerators*», pag. 135 ed. by James F. Ziegler — Plenum Press — New York and London, 1975.

[2] A. P. PATHAK, *Rad. Eff.* **61** (1982) 1 and references therein.

[3] D. S. GEMMEL, *Rev. of Mod. Phys.* **46** (1979), 129.

[4] J. R. CHELIKOWSKY, *Phys. Rev.* **B19** (1979), 686.

[5] D. K. SOOD, *Phys. Lett.* **A68** (1978), 469.

[6] V. A. SINGH, A. ZUNGER, *Phys. Rev.* **B25** (1982), 907.